

Lower lattice thermal conductivity in SbAs than As or Sb monolayer: a first-principles study

San-Dong Guo

School of Physics, China University of Mining and Technology, Xuzhou 221116, Jiangsu, China

Phonon transports of group-VA elements (As, Sb, Bi) monolayer semiconductors have been widely investigated in theory, and Sb monolayer (antimonene) of them has recently been synthesized. In this work, phonon transport of SbAs monolayer is investigated from a combination of first-principles calculations and the linearized phonon Boltzmann equation. It is found that the lattice thermal conductivity of SbAs monolayer is lower than ones of both As and Sb monolayers, and the corresponding sheet thermal conductance is 28.8 WK^{-1} at room temperature. To understand lower lattice thermal conductivity in SbAs monolayer than As and Sb monolayers, group velocities and phonon lifetimes of As, SbAs and Sb monolayers are calculated. Calculated results show that group velocities of SbAs monolayer are between ones of As and Sb monolayers, but phonon lifetimes of SbAs are smaller than ones of both As and Sb monolayers. Hence, low lattice thermal conductivity in SbAs monolayer is attributed to very small phonon lifetimes. Unexpectedly, the ZA branch has very little contribution to the total thermal conductivity, only 2.4%, which is obviously different from ones of As and Sb monolayers with very large contribution. This can be explained by very small phonon lifetimes for ZA branch of SbAs monolayer. The large charge transfer from Sb to As atoms leads strongly polarized covalent bond, being different from As or Sb monolayer. The strongly polarized covalent bond of SbAs monolayer can induce stronger phonon anharmonicity than As or Sb monolayer, leading to lower lattice thermal conductivity. We also consider the isotope and size effects on the lattice thermal conductivity. It is found that isotope scattering produces neglectful effect, and the lattice thermal conductivity with the characteristic length smaller than 30 nm can reach a decrease of about 47%. These results may offer perspectives on tuning lattice thermal conductivity by mixture of multi-elements for applications of thermal management and thermoelectricity, and motivate further experimental efforts to synthesize monolayer SbAs.

PACS numbers: 72.15.Jf, 71.20.-b, 71.70.Ej, 79.10.-n

Keywords: Lattice thermal conductivity; Group velocities; Phonon lifetimes

Email: guosd@cumt.edu.cn

I. INTRODUCTION

Two-dimensional (2D) materials, such as semiconducting transition-metal dichalcogenide¹, group IV-VI², group-VA^{3,4} and group-IV⁵ monolayers, have been widely investigated both in theory and experiment, which have potential applications in high-performance electronics, sensors and alternative energy devices. Recently, stable semiconducting group-VA elements (As, Sb, Bi) monolayers with the graphene-like buckled structure are theoretically predicted³, Sb monolayer (antimonene) of which is prepared successfully on various substrates via van der Waals epitaxy growth^{4,6}. A stibarsen is a natural form of arsenic antimonide (SbAs), which possesses the same layered structure with arsenic and antimony. The counterpart monolayer material of the SbAs bulk with different typical honeycomb polymorph structures has been investigated by the first-principles calculations, and β -SbAs with a graphene-like buckled structure is predicted to be ground state by the cohesive energies⁷. It is found that the biaxial tensile strain can induce semiconductor-topological insulator transition in SbAs monolayer⁷. This implies that monolayer SbAs may play a key role to advance the development of next generation nano-electronics, and may have wide range of potential applications in electronic, quantum and optoelectronic devices.

As is well known, the conduction of heat is a significant

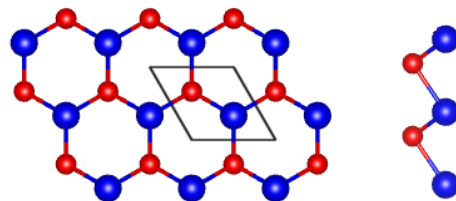


FIG. 1. (Color online) Top and side views of crystal structure of SbAs monolayer, and the unit cell is marked by a black box.

factor to determine the performance of nano-devices. A high thermal conductivity is beneficial to remove the accumulated heat, while a low thermal conductivity is popular in the field of thermoelectric. Therefore, it is interesting and necessary to investigate thermal transport of SbAs monolayer. In theory, thermal transports of lots of 2D materials have been widely investigated by semiclassical Boltzmann transport theory, Green's function based transport techniques and equilibrium molecular dynamics simulations⁸⁻²⁰. The thermal transports of group-VA elements (As, Sb, Bi) monolayers with buckled structure have been predicted¹⁰⁻¹², and the lattice thermal conductivity from As to Bi monolayer monotonously decreases. It is reported that a buckled structure has three conflicting effects: increasing the Debye temperature, suppressing the acoustic-optical scattering and increasing

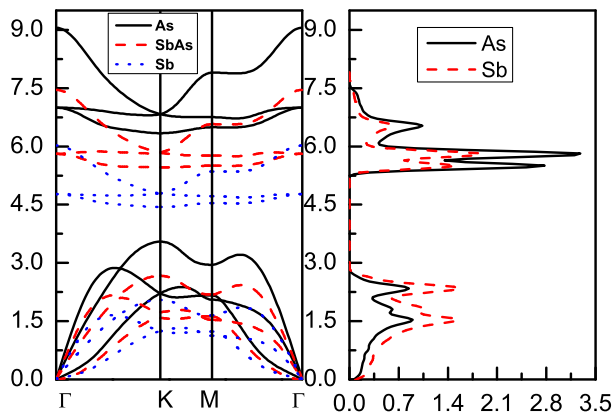


FIG. 2. (Color online) Phonon band structures of As, SbAs and Sb monolayers, together with partial DOS of SbAs monolayer.

the flexural phonon scattering. The former two of them can enhance lattice thermal conductivity, while the third effect can reduce one¹⁴. Strain effects on lattice thermal conductivity also have been studied for various kinds of 2D materials, such as group-IV monolayers^{16,17,19}, antimonene¹⁸ and 2D Penta-Structures monolayers²⁰. It is found that tensile strain can induce strong size effects, and the diverse strain dependence is observed, including monotonously increasing, monotonously decreasing and up-and-down behaviors with strain increasing.

In this work, the phonon transport of SbAs monolayer is investigated based on the single-mode RTA. It is found that the lattice thermal conductivity of SbAs is lower than ones of both As and Sb monolayers with the same buckled honeycomb structure, which is due to shorter phonon lifetimes for SbAs than As or Sb monolayer. The shorter phonon lifetimes is due to large charge transfer from Sb to As atoms, which can induce strongly polarized covalent bond, leading to stronger phonon anharmonicity than As or Sb monolayer. It is noted that the ZA branch of SbAs monolayer has very little contribution to the total thermal conductivity, only 2.4%, being obviously different from ones of As and Sb monolayers with very large contribution. The isotope and size effects on the lattice thermal conductivity are also calculated.

The rest of the paper is organized as follows. In the next section, we shall give our computational details about phonon transport calculations. In the third section, we shall present phonon transport of SbAs monolayer, together with ones of As and Sb monolayer for a comparison. Finally, we shall give our discussions and conclusions in the fourth section.

II. COMPUTATIONAL DETAIL

First-principles calculations are performed within projector augmented-wave method using the VASP code^{21–24}. The generalized gradient approximation

TABLE I. Lattice constants a and buckling parameter h (Å); Thermal sheet conductance κ_L (WK⁻¹).

Name	a	h	κ_L
As	3.61 (3.61 ^{11,14})	1.40 (1.40 ¹⁴)	161.1 (234.8 ¹¹ ,127.4 ¹⁴)
SbAs	3.87 (3.86 ⁷)	1.52 (1.52 ⁷)	28.8
Sb	4.12 (4.12 ^{11,14})	1.65 (1.64 ¹⁴)	46.6 (51.9 ¹¹ ,29.6 ¹⁴)

of Perdew-Burke-Ernzerhof (PBE-GGA) is adopted as exchange-correlation functional²⁴. The unit cells of As, SbAs and Sb monolayers are built with the vacuum region of larger than 16 Å to avoid spurious interaction. A $20 \times 20 \times 6$ q-mesh is used during structural relaxation with a Hellman-Feynman force convergence threshold of 10^{-4} eV/Å. A plane-wave basis set is employed with kinetic energy cutoff of 400 eV. The energy convergence criterion is used, and when the energy difference is less than 10^{-8} eV, the self-consistent calculations are considered to be converged. The lattice thermal conductivity is performed with the single mode RTA and linearized phonon Boltzmann equation, as implemented in the Phono3py code²⁵. The interatomic force constants (IFCs) are calculated by the finite displacement method. The second order harmonic and third order anharmonic IFCs are calculated by using a $5 \times 5 \times 1$ supercell and a $4 \times 4 \times 1$ supercell, respectively. Using the harmonic IFCs, phonon dispersion can be calculated by Phonopy package²⁶, determining the allowed three-phonon scattering processes, group velocity and specific heat. Based on third-order anharmonic IFCs, the phonon lifetimes can be attained from the three-phonon scattering rate. To compute lattice thermal conductivities, the reciprocal spaces of the primitive cells are sampled using the $50 \times 50 \times 2$ meshes. For 2D material, the calculated lattice thermal conductivity depends on the length of unit cell used in the calculations along z direction²⁷. The lattice thermal conductivity should be normalized by multiplying Lz/d , in which Lz is the length of unit cell along z direction and d is the thickness of 2D material, but the d is not well defined. In this work, the length of unit cell (18 Å) along z direction is used as the thickness of As, SbAs and Sb monolayers. To make a fair comparison between various 2D monolayers, the thermal sheet conductance can be used, defined as $\kappa \times d$.

III. MAIN CALCULATED RESULTS AND ANALYSIS

The β -SbAs monolayer with a graphenelike buckled honeycomb structure is similar to those of group-VA and group-IV monolayers, and the schematic crystal structure is shown in Figure 1. The SbAs monolayer (No.156) has lower symmetry compared with As and Sb monolayers (No.164) due to the different types of atoms constituting the compound. Firstly, the lattice constants are

optimized, and the resulting $a=b=3.867$ Å and buckling parameter $h=1.515$ Å, which are very close to previous theoretical values⁷. The lattice constants and buckling parameter h in this or previous works^{7,11,14} are summarized in Table I for As, SbAs and Sb monolayers. It is expected that both lattice constants and buckling parameter of SbAs monolayer are greater than ones of As monolayer, but less than ones of Sb monolayer.

The phonon dispersions of As, SbAs and Sb monolayers in high symmetry directions are plotted in Figure 2, together with partial density of states (DOS) of SbAs monolayer. Due to containing two atoms in their unit cell, 3 acoustic and 3 optical phonon branches can be observed. Due to buckling of As, SbAs and Sb monolayers, their out-of-plane acoustic modes have coupling with the in-plane longitudinal acoustic (LA) and transversal acoustic (TA) modes. However, the out-of-plane acoustic modes are still marked with ZA modes. It is clearly seen that LA and TA branches are linear near the Γ point, while ZA branch deviates from linearity, which shares the general feature of 2D materials^{8–20}. It is clearly seen that both acoustic and optical branches overall move downward from As to SbAs to Sb monolayer, and the widths of acoustic and optical branches gradually become narrow. The maximal acoustic vibration frequency (MAVF) is 3.55 THz, 2.67 THz and 2.05 THz from As to SbAs to Sb monolayer, and the width of optical branches (WOOB) is 2.71 THz, 1.99 THz and 1.58 THz, respectively. The low MAVF and narrow WOOB mean small group velocities, which is benefit to low thermal conductivity. The Debye temperature θ_D can be calculated with the MAVF by $\theta_D = h\nu_m/k_B$ ^{8,9}, where h , k_B are the Planck constant and Boltzmann constant. The calculated θ_D for As, SbAs and Sb monolayers is 170.36, 128.13 and 98.38 K, respectively. A phonon band gap between acoustic and optical branches can be observed, and the corresponding value is 2.79 THz, 2.79 THz and 2.39 THz from As to SbAs to Sb monolayer. The gaps of As and Sb monolayers are due to the violation of reflection symmetry selection rule in the harmonic approximation¹⁴, while the gap of SbAs is due to not only the violation of reflection symmetry selection rule but also mass differences between the constituent atoms^{28,29}. Therefore, the gap of As monolayer is the same with that of SbAs monolayer, not like that the gap gradually decreases from As to Sb to Bi monolayer. According to partial DOS of SbAs monolayer, the optical modes of SbAs are mainly from As vibrations, while the acoustic branches are mainly due to the vibrations of Sb.

The lattice thermal conductivities of As, SbAs and Sb monolayers are calculated with RTA method, which are shown in Figure 3. The room-temperature lattice thermal conductivity of As, SbAs and Sb monolayers is $8.95 \text{ Wm}^{-1}\text{K}^{-1}$, $1.60 \text{ Wm}^{-1}\text{K}^{-1}$ and $2.59 \text{ Wm}^{-1}\text{K}^{-1}$, respectively, with the same thickness d (18 Å). To make a fair comparison between various 2D materials, their thermal sheet conductance²⁷ is 161.1 WK^{-1} , 28.8 WK^{-1} and

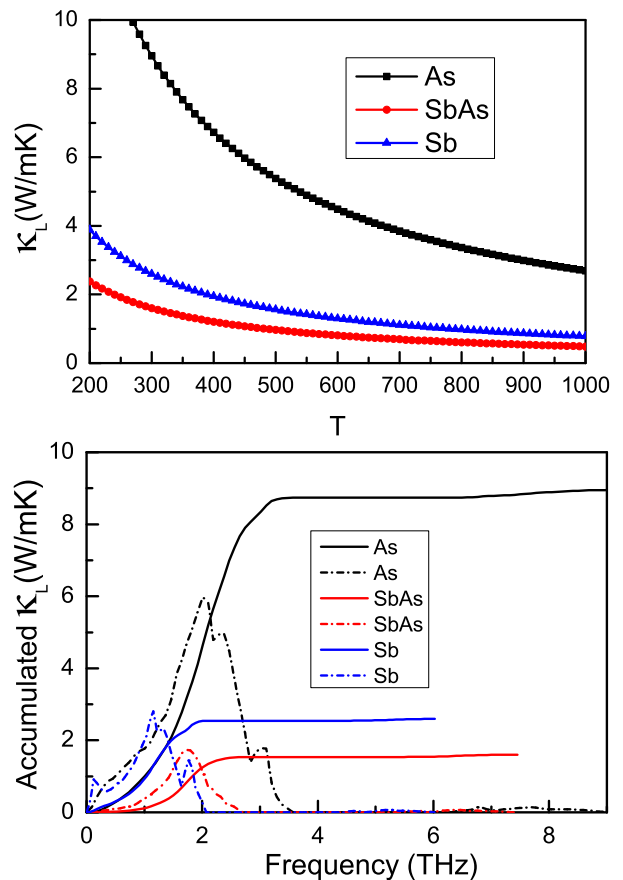


FIG. 3. (Color online) Top: the lattice thermal conductivities of As, SbAs and Sb monolayers as a function of temperature. Bottom: the accumulated lattice thermal conductivities with respect to frequency (solid lines), and the derivatives (short dash dot lines).

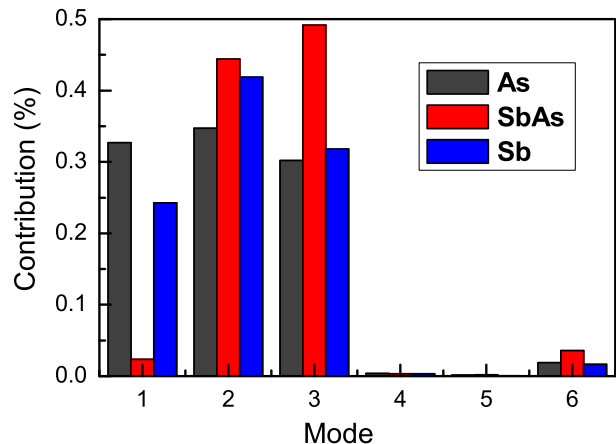


FIG. 4. (Color online) The phonon modes contributions toward total lattice thermal conductivity of As, SbAs and Sb monolayers (300 K).

46.6 WK^{-1} , respectively. The room-temperature thermal sheet conductances are listed in Table I, together

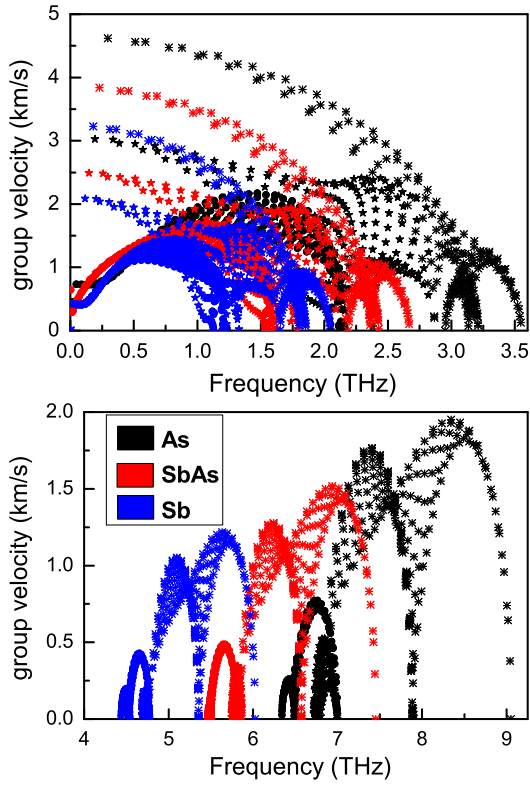


FIG. 5. (Color online) The phonon mode group velocities of As, SbAs and Sb monolayers in the first Brillouin zone. Top: the ZA (circle symbol), TA (star symbol) and LA (star (*) symbol) acoustic branches; Bottom: the first (circle symbol), second (star symbol) and third (star (*) symbol) optical branches.

with available previous theoretical values of As and Sb monolayers^{11,14}, which have been converted into thermal sheet conductances. Our calculated values are in the range of previous ones. The SbAs monolayer can be attained by using As (Sb) atoms to replace one sublayer of Sb (As) monolayer. It is expected that the lattice thermal conductivity of SbAs monolayer should be between ones of As and Sb monolayers. However, it is clearly seen that the lattice thermal conductivity of SbAs monolayer is lower than any of ones of As and Sb monolayers. The cumulative lattice thermal conductivity and the derivatives are also plotted in Figure 3 at room temperature. The acoustic branches of As, SbAs and Sb monolayers provide a contribution of 97.6%, 95.9% and 98.0%, respectively, which meets the usual picture that acoustic branches dominate lattice thermal conductivity. It is found that the slope of cumulative lattice thermal conductivity of SbAs monolayer is smaller than ones of As and Sb monolayers, which means that the low-frequency acoustic phonons of SbAs monolayer have very little contribution to thermal conductivity. To further examine the relative contributions of every phonon modes to the total lattice thermal conductivity, the phonon modes contributions toward total lattice thermal conductivity of

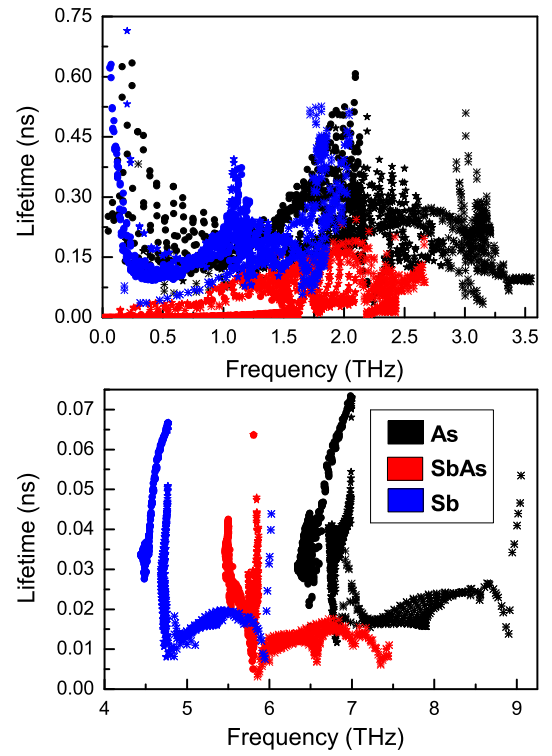


FIG. 6. (Color online) The phonon mode lifetimes of As, SbAs and Sb monolayers in the first Brillouin zone. Top: the ZA (circle symbol), TA (star symbol) and LA (star (*) symbol) acoustic branches; Bottom: the first (circle symbol), second (star symbol) and third (star (*) symbol) optical branches.

As, SbAs and Sb monolayers (300 K) are shown in Figure 4. It is found that ZA branch provides very large contribution for As and Sb monolayers, but very little contribution for SbAs monolayer, only 2.4%. However, the TA and LA branches have larger contribution for SbAs monolayer than As and Sb monolayers. Especially, the LA branch provides almost half of lattice thermal conductivity for SbAs monolayer, up to 49.1%. It is clearly seen that the third optical branch has relatively obvious contribution.

To identify the underlying mechanism of lower lattice thermal conductivity in SbAs monolayer than As and Sb monolayers, phonon mode group velocities of As, SbAs and Sb monolayers are calculated, which are shown in Figure 5. For all branches, it is clearly seen that most of group velocities become small from As to SbAs to Sb monolayer, which can lead to decreasing lattice thermal conductivity. From As to SbAs to Sb monolayer, the largest group velocity changes from 2.17 kms^{-1} to 1.69 kms^{-1} to 1.45 kms^{-1} for ZA branch, from 3.03 kms^{-1} to 2.49 kms^{-1} to 2.08 kms^{-1} for TA branch, from 4.62 kms^{-1} to 3.84 kms^{-1} to 3.23 kms^{-1} for LA branch. Therefore, the changes of group velocities can not explain lower lattice thermal conductivity in SbAs monolayer than As and Sb monolayers. In the single-mode RTA method, phonon lifetimes are merely proportional

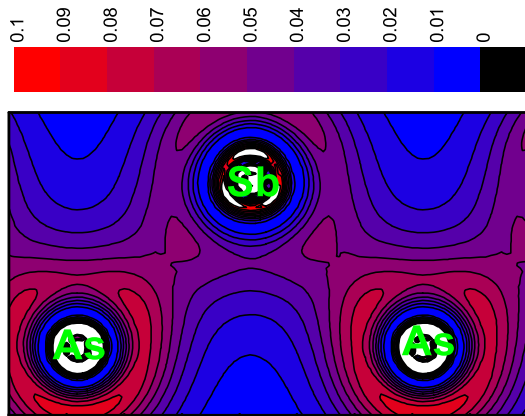


FIG. 7. (Color online) The charge density distributions of SbAs (unit: $|e|/\text{bohr}^3$).

to lattice thermal conductivity²⁵, which can be calculated by three-phonon scattering rate from third-order anharmonic IFCs. The phonon lifetimes of As, SbAs and Sb monolayers are plotted in Figure 6. For all phonon branches, most of phonon lifetimes become large from SbAs to Sb to As monolayer, which means that SbAs monolayer has lowest lattice thermal conductivity. It is clearly seen that most of phonon lifetimes of ZA branch for SbAs monolayer are very small, which leads to very little contributions toward total lattice thermal conductivity of SbAs monolayer for ZA branch. Because acoustic branches have larger group velocities and phonon lifetimes than optical ones, acoustic branches dominate the lattice thermal conductivity. According to group velocities, the lattice thermal conductivity of SbAs monolayer should be between ones of As and Sb monolayers. However, SbAs monolayer has the lowest one by analyzing phonon lifetimes. So, the short phonon lifetimes lead to lower lattice thermal conductivity in SbAs monolayer than As and Sb monolayers.

The distribution of electrons in real space can be described by the charge density distributions, which determines the bond characteristics between atoms. The charge density distributions of SbAs monolayer is shown in Figure 7. For As and Sb monolayers, there is no charge transfer among As or Sb atoms due to the same atom types to form bond. But for SbAs monolayer, from Sb to As atom, the charge density distinctly increases, which indicates that charge transfer between Sb and As atoms occurs. This can be understood by considering the different electronegativity between As (2.18) and Sb (2.05) atoms. The charge transfer from Sb to As atom can give rise to the relatively strongly polarized covalent bond. The inhomogeneous distribution of charge density of monolayer SbAs can induce larger anharmonicity than As and Sb monolayers, which leads to stronger intrinsic phonon-phonon scattering, driving the lower lattice thermal conductivity of monolayer SbAs than As and Sb monolayers. Similar results can also be found in SiC and GaN monolayers^{9,30}

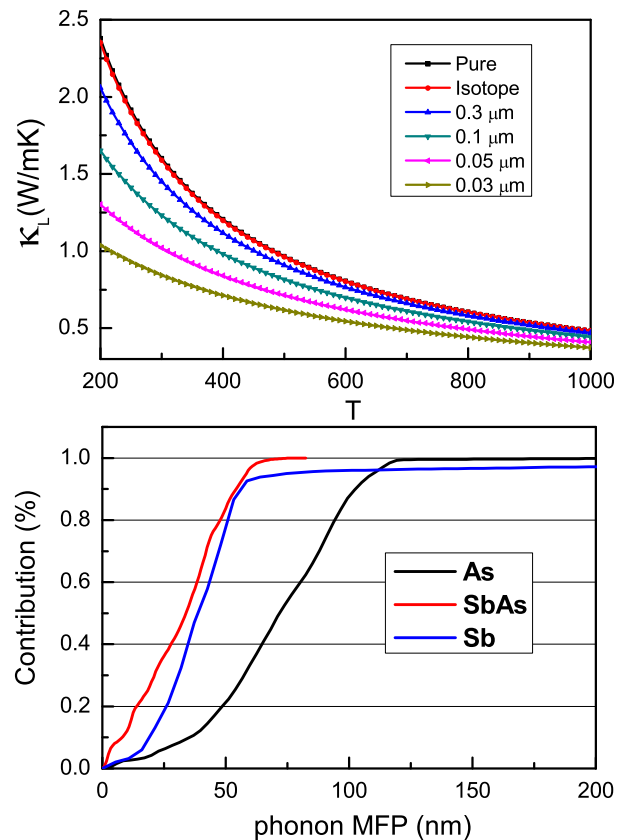


FIG. 8. (Color online) Top: the lattice thermal conductivities of infinite (Pure and Isotope) and finite-size (0.3, 0.1, 0.05 and 0.03 μm) monolayer SbAs as a function of temperature; Bottom: the cumulative lattice thermal conductivity of As, SbAs and Sb monolayers divided by their total lattice thermal conductivity with respect to phonon MFP at room temperature.

According to the formula given by Shin-ichiro Tamura³¹, the phonon-isotope scattering is considered. Calculated results show very insensitivity of lattice thermal conductivity to isotopes, as shown in Figure 8. A most simple boundary scattering treatment is adopted, whose scattering rate can be attained by v_g/L , where v_g , L are the group velocity and the boundary MFP, respectively. The lattice thermal conductivities of finite-size (0.3, 0.1, 0.05 and 0.03 μm) SbAs monolayer as a function of temperature are plotted in Figure 8. As the sample size of SbAs decreases, the lattice thermal conductivity decreases, which is due to enhanced boundary scattering. For the 0.3, 0.1, 0.05 and 0.03 μm cases, the room-temperature lattice thermal conductivity of SbAs monolayer is reduced by about 9.50%, 23.13%, 36.33% and 47.40% compared with infinite (Pure) case.

The thermal conductivity spectroscopy technique can measure MFP distributions over a wide range of length scales³². Therefore, cumulative lattice thermal conductivity divided by total lattice thermal conductivity of As, SbAs and Sb monolayers with respect to phonon MFP,

at room temperature, are plotted in in [Figure 8](#), which can be used to study size effects in heat conduction. As the MFP increases, the cumulative lattice thermal conductivity divided by total lattice thermal conductivity increases, and then approaches one. From As to SbAs to Sb monolayer, the corresponding critical MFP changes from 124 nm to 68 nm to 432 nm. It has been proved that strain can induce very strong size effects on lattice thermal conductivity of Sb monolayer¹⁸, which means that critical MFP significantly depends on lattice constants. When the lattice thermal conductivity is reduced to 60% by nanostructures, the characteristic length varies from 80 nm to 38 nm to 44 nm from As to SbAs to Sb monolayer.

IV. DISCUSSIONS AND CONCLUSION

Compared with the planar geometry of graphene, it is demonstrated that a buckled structure has conflicting effects on lattice thermal conductivity¹⁴. On the one hand, buckled structure can increase lattice thermal conductivity by the formation of an acoustic-optical gap, suppressing $A+A \leftrightarrow O$ scattering. On the other hand, it can reduce one by breaking the out-of-plane symmetry, increasing anharmonic phonon scattering. The As, SbAs and Sb monolayers all possess buckled structure. The buckling parameter h monotonically increases from As to SbAs to Sb monolayer, and the acoustic-optical gap of SbAs monolayer is larger than that of Sb monolayer. Therefore, the trend of lattice thermal conductivity from As to SbAs to Sb monolayer cannot be addressed by conflicting effects caused by buckled structure. Based on the formula proposed by Slack³³, the average atomic mass, interatomic bonding, crystal structure and anharmonicity determine the lattice thermal conductivity of a material. Calculated results show that the anharmonicity can explain the trend of lattice thermal conductivity from As to SbAs to Sb monolayer. According to [Figure 7](#), the charge transfer of monolayer SbAs can induce larger anharmonicity than As and Sb monolayers, which produces stronger intrinsic phonon-phonon scattering, leading to shorter phonon lifetimes ([Figure 6](#)). This drives the lower lattice thermal conductivity of monolayer SbAs than As and Sb monolayers.

Strain has been proved to be very effective to tune lattice thermal conductivities of various 2D materials^{16–20}. For planar structure, for example graphene, the reflec-

tion symmetry selection rule strongly restricts anharmonic phonon scattering, leading to very high lattice thermal conductivity¹⁴. Tensile strain can make a buckled structure turn into a planar structure like penta-SiN₂, predicted by the first-principles calculations²⁰. When the structure becomes perfectly planar, the lattice thermal conductivity of penta-SiN₂ suddenly jumps up by 1 order of magnitude. In fact, the buckled structure of Bi monolayer becomes perfectly planar, which has been experimentally achieved³⁴. Therefore, it is possible for SbAs monolayer to achieve high thermal conductivity by tensile strain, which can dissipate heat efficiently in SbAs monolayer-based nano-electronics devices. The As, Sb, Bi and SbAs monolayers with the graphene-like buckled structure are predicted to stable in theory^{3,7}. The Sb monolayer (antimonene) has been achieved in experiment^{4,6}, and it has been proved that tensile strain can enhance structural stability¹⁸ for Sb monolayer, which provides guidance on fabrication of these monolayers. The Bi monolayer has been successfully synthesized by tensile strain³⁴. Therefore, it is possible to achieve SbAs monolayer in experiment by tensile strain.

In summary, the lattice thermal conductivities of SbAs monolayer, together with As and Sb monolayers, are performed by solving the linearized phonon Boltzmann equation within the single-mode RTA. Calculated results show that the lattice thermal conductivity of SbAs is lower than ones of both As and Sb monolayers, which is due to the shorter phonon lifetimes for SbAs than As or Sb monolayer. The short phonon lifetimes is due to charge transfer from Sb to As atoms, being different from that in As or Sb monolayer, which leads to strong intrinsic phonon-phonon scattering. The size dependence of lattice thermal conductivity is studied, which can provide guidance on designing nanostructures. This work provides insight into phonon transport in SbAs monolayer, and offers new idea on tuning lattice thermal conductivity by mixture of multi-elements.

ACKNOWLEDGMENTS

This work is supported by the National Natural Science Foundation of China (Grant No.11404391). We are grateful to the Advanced Analysis and Computation Center of CUMT for the award of CPU hours to accomplish this work.

¹ M. Chhowalla, H. S. Shin, G. Eda, L. J. Li, K. P. Loh and H. Zhang, *Nature Chemistry* **5**, 263 (2013).

² R. X. Fei, W. B. Li, J. Li and L. Yang, *Appl. Phys. Lett.* **107**, 173104 (2015).

³ S. L. Zhang M. Q. Xie, F. Y. Li, Z. Yan, Y. F. Li, E. J. Kan, W. Liu, Z. F. Chen, H. B. Zeng, *Angew. Chem.* **128**, 1698 (2016).

⁴ J. P. Ji, X. F. Song, J. Z. Liu et al., *Nat. Commun.* **7**, 13352 (2016).

⁵ S. Balendhran, S. Walia, H. Nili, S. Sriram and M. Bhaskaran, *small* **11**, 640 (2015).

⁶ P. Ares, F. A. Galindo, D. R. S. Miguel et al., *Adv. Mater.* **28**, 6332 (2016).

⁷ S. L. Zhang, M. Q. Xie, B. Cai, H. J. Zhang, Y. D. Ma, Z.

- F. Chen, Z. Zhu, Z. Y. Hu, and H. B. Zeng, *Phys. Rev. B* **93**, 245303 (2016).
- ⁸ H. M. Wang, G. Z. Qin, G. J. Li, Q. Wang and M. Hu, *Phys. Chem. Chem. Phys.* **19**, 12882 (2017).
- ⁹ Z. Z. Qin, G. Z. Qin, X. Zuo, Z. H. Xiong and M. Hu, *Nanoscale* **9**, 4295 (2017).
- ¹⁰ S. D. Wang, W. H. Wang and G. J. Zhao, *Phys. Chem. Chem. Phys.* **18**, 31217 (2016).
- ¹¹ G. H. Zheng, Y. L. Jia, S. Gao and S. H. Ke, *Phys. Rev. B* **94**, 155448 (2016).
- ¹² D. C. Zhang, A. X. Zhang, S. D. Guo and Y. F. Duan, *RSC Adv.* **7**, 24537 (2017).
- ¹³ S. D. Guo, *J. Mater. Chem. C* **4**, 9366 (2016).
- ¹⁴ B. Peng, D. Q. Zhang, H. Zhang, H. Z. Shao, G. Ni, Y. Y. Zhu and H. Y. Zhu, *Nanoscale* **9**, 7397 (2017).
- ¹⁵ H. Y. Lv, W. J. Lu, D. F. Shao, H. Y. Lub and Y. P. Sun, *J. Mater. Chem. C* **4**, 4538 (2016).
- ¹⁶ H. Xie, T. Ouyang, E. Germaneau, G. Z. Qin, M. Hu and H. Bao, *Phys. Rev. B* **93**, 075404 (2016).
- ¹⁷ Y. D. Kuang, L. Lindsay, S. Q. Shic and G. P. Zheng, *Nanoscale* **8**, 3760 (2016).
- ¹⁸ A. X. Zhang, J. T. Liu, S. D. Guo and H. C. Li, *Phys. Chem. Chem. Phys.* **19**, 14520 (2017).
- ¹⁹ L. Lindsay, Wu Li, J. Carrete, N. Mingo, D. A. Broido and T. L. Reinecke, *Phys. Rev. B* **89**, 155426 (2014).
- ²⁰ H. K. Liu, G. Z. Qin, Y. Lin and M. Hu, *Nano Lett.* **16**, 3831 (2016).
- ²¹ G. Kresse, *J. Non-Cryst. Solids* **193**, 222 (1995).
- ²² G. Kresse and J. Furthmüller, *Comput. Mater. Sci.* **6**, **15** (1996).
- ²³ G. Kresse and D. Joubert, *Phys. Rev. B* **59**, 1758 (1999).
- ²⁴ J. P. Perdew, K. Burke and M. Ernzerhof, *Phys. Rev. Lett.* **77**, 3865 (1996).
- ²⁵ A. Togo, L. Chaput and I. Tanaka, *Phys. Rev. B* **91**, 094306 (2015).
- ²⁶ A. Togo, F. Oba, and I. Tanaka, *Phys. Rev. B* **78**, 134106 (2008).
- ²⁷ X. F. Wu, V. Varshney et al., *Chem. Phys. Lett.* **669**, 233 (2017).
- ²⁸ L. Lindsay, D. A. Broido and T. L. Reinecke, *Phys. Rev. Lett.* **111**, 025901 (2013).
- ²⁹ X. Gu and R. Yang, *Appl. Phys. Lett.* **105**, 131903 (2014).
- ³⁰ S. D. Guo, J. T. Liu, A. X. Zhang and H. C. Li, arXiv:1706.01025 (2017).
- ³¹ S.I. Tamura, *Phys. Rev. B*, **27**, 858 (1983).
- ³² A. J. Minnich, J. A. Johnson, A. J. Schmidt, K. Esfarjani, M. S. Dresselhaus, K. A. Nelson and G. Chen, *Phys. Rev. Lett.* **107**, 095901 (2011).
- ³³ G. A. Slack, *J. Phys. Chem. Solids* **34**, 321 (1973).
- ³⁴ F. Reis, G. Li, L. Dudy, M. Bauernfeind, S. Glass, W. Hanke, R. Thomale, J. Schäfer and R. Claessen, *Science* 10.1126/science.aai8142 (2017).